The International Journal of Advanced Manufacturing Technology (2021) 116:1925–1936
https://doi.org/10.1007/s00170-021-07452-1

ORIGINAL ARTICLE

Effect of yield criterion and variable elastic modulus on springback prediction of Ti-6Al-4V sheet V-shaped bending

Zijian Liu[1,2] · Lidong Ma[1,2,3] · Zhijuan Meng[4] · Peiyu Liu[1,2] · Yukang Du[1,2]

Received: 23 February 2021 / Accepted: 8 June 2021 / Published online: 5 July 2021

Abstract

In recent years, Ti-6Al-4V titanium alloy has been widely used in many fields because of its excellent material properties. However, the complex properties of Ti-6Al-4V titanium alloy make the common material constitutive model no longer applicable. It is difficult to accurately analyze the deformation process of Ti-6Al-4V titanium alloy in theoretical analysis or numerical simulation. In this paper, we take Ti-6Al-4V titanium alloy as the research object, and the change of elastic modulus of Ti-6Al-4V titanium alloy was studied. A mathematical model of titanium alloy variable elastic modulus was established. Based on the YLD2000-2D yield criterion and the mathematical model of variable elastic modulus, the constitutive model of Ti-6Al-4V titanium alloy was established. We have carried out the numerical simulation and field experiment of V-bending springback of Ti-6Al-4V titanium alloy sheet. The springback prediction accuracy of three different constitutive models was compared and analyzed. The influence of yield criterion and elastic modulus on springback prediction of titanium alloy V-bending was studied. The results show that the constitutive model established in this paper significantly improved the springback prediction accuracy of the numerical simulation of titanium alloy sheet bending. This work has made a great contribution to the field of titanium alloy bending forming.

Keywords Ti-6Al-4V · Bending forming · Springback prediction · Variable elastic modulus · Yield criterion

1 Introduction

Ti-6Al-4V high-strength titanium alloy is widely used in aerospace, shipbuilding, and automotive industries because of its light weight, high strength, heat resistance, and corrosion resistance [1–4]. Ti-6Al-4V alloy has low elastic modulus and high strength, which cause serious springback phenomenon during bending forming. Predicting the springback in forming is one of the key issues to ensure product quality.

Many scholars have done a lot of research on the theory of bending springback. Zhao et al. [5] established the plane-bending elastic complex equation and successfully applied it to the diameter expansion and rounding process. On this basis, Zhao et al. also studied the prediction and control of springback during the refurbishment of large pipe ends, and the springback analysis of the profile plane tensile bending was studied through the loading method of pretension and moment [6, 7]. Liu et al. [8] proposed an analysis method for predicting springback and residual stress distribution in thick plate multi-point forming. Ma et al. [9] analyzed the five-point bending process and springback process of the FFX precast section of ERW tube and established a five-point bending springback mechanical model. Wu et al. [10] took the high-strength steel thick plates as the research object and analyzed the influencing parameters of springback in cold bending forming through numerical simulation methods. However, the theoretical analysis method has a small application range, and it is difficult to solve the springback problem of anisotropic materials.

✉ Lidong Ma
mald@tyust.edu.cn

1 Coordinative Innovation Center of Taiyuan Heavy Machinery Equipment, Taiyuan University of Science and Technology, Taiyuan 030024, China

2 School of Materials Science and Engineering, Taiyuan University of Science and Technology, Taiyuan 030024, China

3 School of Mechanical Engineering, Taiyuan University of Science and Technology, Taiyuan 030024, China

4 School of Applied Sciences, Taiyuan University of Science and Technology, Taiyuan 030024, China

Finite element simulation is also one of the important methods to predict the springback of materials. At present, many scholars use finite element simulation methods to predict springback in the metal bending process. Numerical simulation results and actual results always have a certain error, which is related to the model, meshing, material constitutive setting, boundary condition setting, etc., of which the material constitutive model is particularly important. In 1989, Barlat et al. [11] proposed an anisotropic yield criterion, which is suitable for plane stress conditions and can describe the in-plane anisotropy of sheet metal deformation. In 2003, Barlat et al. [12] also proposed the YLD2000-2D yield criterion and applied it to the finite element analysis of the aluminum alloy sheet forming process. Naofal et al. [13] studied the springback prediction of the sheet roll forming process based on the Y-U hardening model and variable elastic modulus. The results show that the hardening model and changes in the elastic modulus have a great influence on the springback prediction. Jung et al. [14] took high-strength steel (AHSS) as the research object, developed an anisotropic elastoplastic constitutive model, and applied it to predict springback during U-bending. Badr et al. [15–17] proposed the roll forming processing of Ti-6Al-4V titanium alloy at room temperature and an anisotropic elastoplastic constitutive model. The constitutive model has higher accuracy in predicting the Bauschinger effect and transient hardening behavior of Ti-6Al-4V thin plate samples at room temperature. On this basis, they also studied the influence of rolling forming process parameters on Ti-6Al-4V bending springback at room temperature. Yang et al. [18] studied the springback of TC4 titanium alloy under hot stamping condition by means of experiment and numerical analysis. Mulidrán et al. [19] used Hill48 and Barlat yield criteria in combination with Ludwik's and Swift's hardening models to simulate the V-shaped bending springback process of DC06. They also used numerical simulation to predict the springback of the hat-shaped part made of advanced high-strength dual-phase steel HCT600X+Z, and these numerical predictions were performed with the use of various combinations of material models [20].

With the advancement of science and technology and the continuous development of the manufacturing industry, people have put forward higher requirements for the accuracy of springback prediction. The elastic modulus changes during the molding process, which affects the accuracy of springback prediction. Morestin et al. [21] found through experiments that when the plastic strain only reaches 5%, the elastic modulus can be reduced to more than 10% of the initial value, and the developed software calculates the springback in the stamping process. The software considers the change of elastic modulus. The calculated result is very close to the experimental value. Yoshida et al. [22] studied the material properties of DP590 high-strength steel and found that when the pre-strain was increased, the elastic modulus showed a rapid downward trend and proposed the Y-U hardening model and the variable elastic modulus mathematical model. Liu et al. [23] took ultra-high-strength steel as the research object, proposed a mathematical model that considers the changes in Young's modulus, and applied it to three-dimensional finite element analysis (FEA) to simulate the cold rolling forming process. Compared with the constitutive model of Swift material, the springback accuracy calculated by using nonlinear elastic modulus is improved by 18%. Sun et al. [24] established a QPE (quasi-plastic-elastic) model to describe the nonlinear change of elastic modulus for the bending springback behavior of materials. This model improves the prediction accuracy of springback.

This paper takes Ti-6Al-4V titanium alloy as the research object, through uniaxial tensile experiment and cycle loading-unloading-loading experiment, the material anisotropy and the elastic modulus change rule during material deformation is studied. A mathematical model of variable elastic modulus is established. Based on the variable elastic modulus mathematical model and YLD2000-2D yield criterion, the material constitutive model subroutine was established. The Abaqus simulation software Umat (user-defined material) subroutine interface was used to embed the custom constitutive model into the finite element model. Numerical simulation of V-bending springback of Ti-6Al-4V titanium alloy sheet with different constitutive models was carried out. Finally, we conducted a Ti-6Al-4V titanium alloy V-shaped bending experiment and compared the experimental results with the simulated results.

2 Material performance experiment

2.1 Material selection

Ti-6Al-4V titanium alloy is widely used in various industries due to its good corrosion resistance and high strength. It is currently a hot metal researched by scholars in the world. The chemical composition of Ti-6Al-4V titanium alloy selected in this paper is shown in Table 1.

2.2 Quasi-static uniaxial tensile test

In order to measure the material properties and anisotropy coefficient of Ti-6Al-4V titanium alloy, we conducted a quasi-static uniaxial tensile test. As shown in Fig. 1, the

Table 1 Material chemical composition

Element	Ti	Fe	C	N	H	O	A1	V
%	Rest	0.30	0.08	0.05	0.015	0.20	6.50	4.50

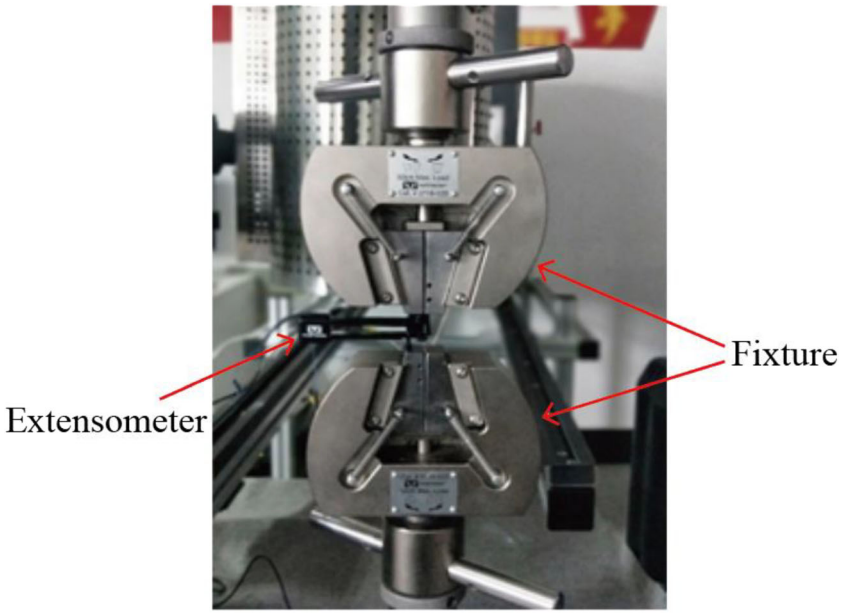

Fig. 1 Instron-5969 universal material testing machine

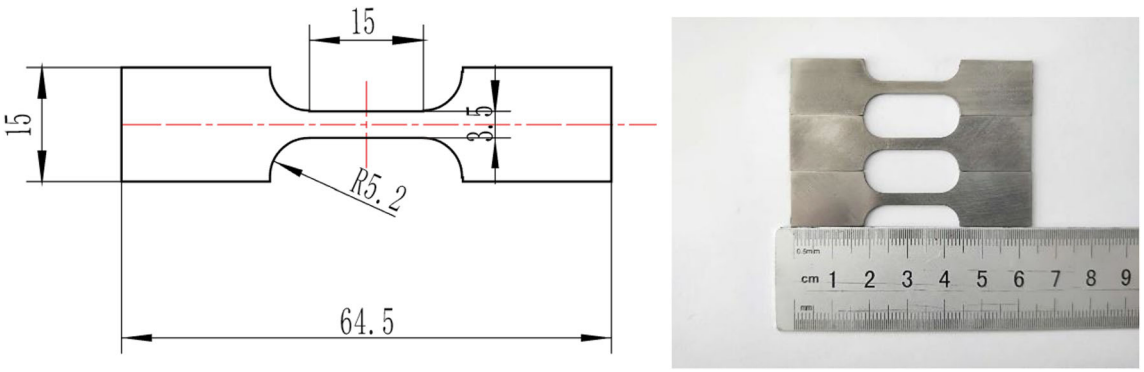

Fig. 2 The size of the tensile specimen

experiment was carried out on the Instron-5969 universal material testing machine (load 50 kN).

We have carried out tensile experiments on the three directions of RD (rolling direction), DD (diagonal direction), and TD (transverse direction) of the material. According to the experimental requirements, we made tensile specimens. The size of the tensile specimen is shown in Fig. 2. As shown in Fig. 3, tensile specimens were sampled at 0°, 45°, and 90° in the rolling

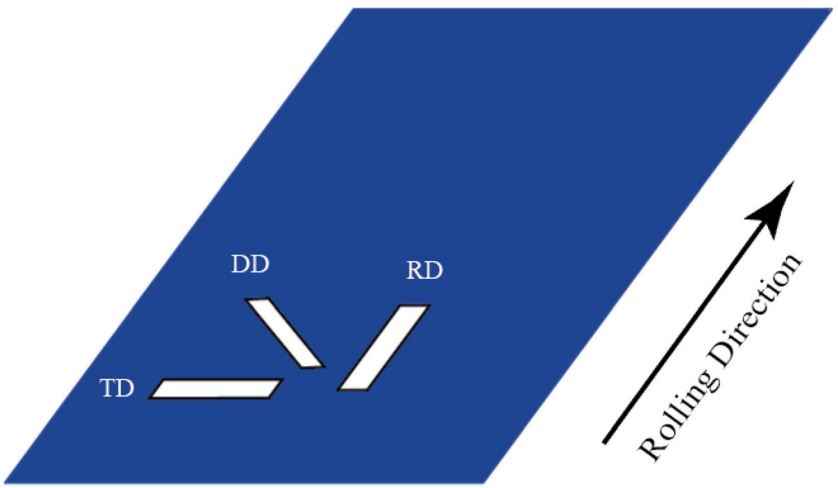

Fig. 3 Schematic diagram of tensile specimen cutting method

direction of the sheet. This experiment is carried out at room temperature, and the stretching rate is 0.01 mm/s. This experiment uses a contact extensometer to measure deformation.

2.3 Cycle loading-unloading-loading experiment

In order to determine the elastic modulus of Ti-6Al-4V titanium alloy under different plastic strains, we carried out cycle loading-unloading-loading experiments. The experiment is also carried out on the Instron-5969 universal material testing machine. The experimental conditions and tensile specimen are the same as the uniaxial quasi-static tensile experiment. The specific experimental steps of the cycle loading-unloading-loading experiment are as follows. Firstly, stretch the specimen to the required initial pre-strain, and then unload the stress to zero. The specimen was stretched to the second specific strain and released again when the loading-unloading cycle was accomplished. This cycle is continued until the maximum preset strain value is achieved. The pre-strain is set to 0.8%, 1.0%, 1.5%, 2%, 2.5%, 3.3%, 4.1%, 5.1%, 6.1%, 7.1%, 8.1%, and 9.1%. We tested the patterns in the three directions of RD, DD, and TD. (The elongation rate of TD direction is low. In order to prevent the contact extensometer from being damaged, the pre-strain value of the pattern in the TD direction is only set to 7.1%.)

The stress-strain curves in the three directions of RD, DD, and TD measured by the cycle loading-unloading-loading experiment are shown in Fig. 4.

2.4 Analysis of experimental results

The stress-strain curves of Ti-6Al-4V titanium alloy in RD, DD, and TD directions are obtained by uniaxial quasi-static tensile test, as shown in Fig. 5.

The elastic modulus, 0.2% offset yield strength, ultimate tensile strength, total elongation, and plastic strain ratio (r value) of Ti-6Al-4V titanium alloy of RD, DD, and TD measured in uniaxial tensile test are shown in Table 2.

The r-value is calculated according to the following formula.

$$r = \frac{\varepsilon_w}{\varepsilon_t} = \frac{\ln \frac{\omega}{\omega_0}}{\ln \frac{t}{t_0}}, \tag{1}$$

where ε_w and ε_t are the strain in the width direction and the thickness direction respectively. ω_0 and ω are the initial width and final width, and t_0 and t are the initial thickness and final thickness of the specimen.

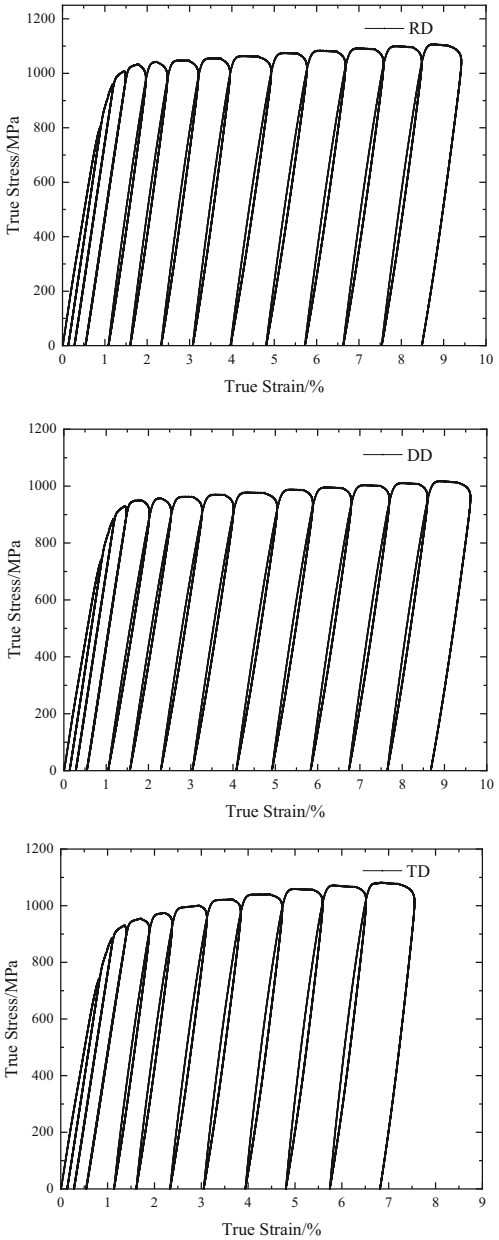

Fig. 4 Cycle loading-unloading-loading experiment stress-strain curves

3 Definition of elastic modulus change

Generally, the value of elastic modulus is the slope of the linear segment in the stress-strain curve. According to the cycle load-unload-load experiment data in the previous section, we can find that the reloaded loading curve has hysteresis characteristics and is no longer linear. The calculation method of elastic modulus can no longer use the previous method. Therefore, some scholars have proposed three calculations of elastic modulus: loaded modulus, unloaded modulus, and chord modulus. The unloading modulus is the slope of the connecting line in the first half of the unloading curve. The loading modulus is the

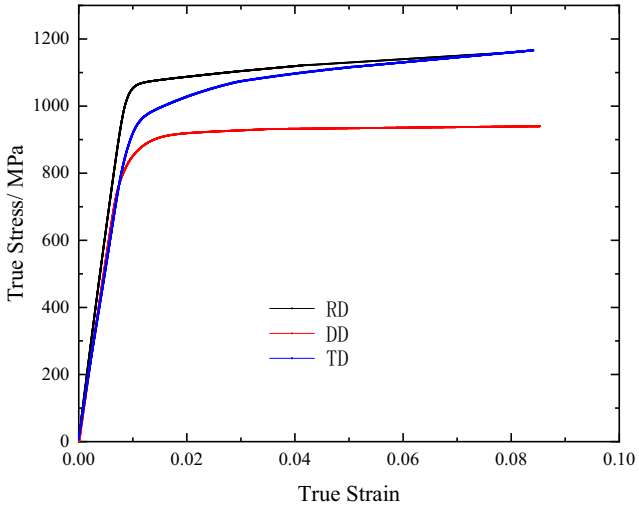

Fig. 5 Ti-6Al-4V titanium alloy stress-strain curves

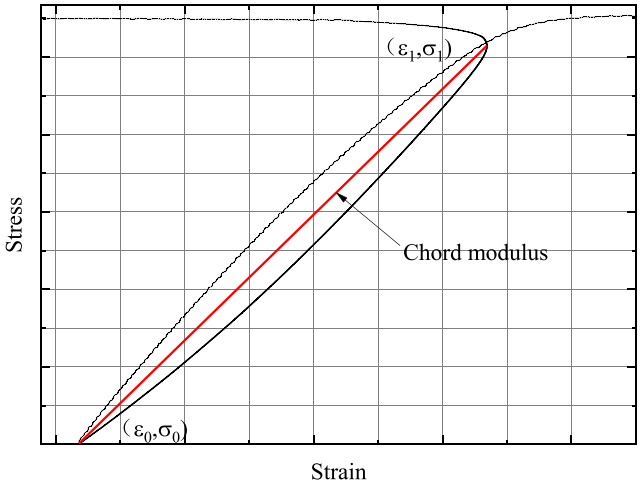

Fig. 6 Schematic diagram of chord modulus calculation method

slope of the line connecting the first half of the secondary loading curve. The chord modulus is the slope of the line connecting the previous maximum strain point and the next initial strain point, as shown in Fig. 6. This paper selects the calculation method of chord modulus to calculate the elastic modulus value in the load-unload-load curve. The formula for calculating string modulus is as follows.

$$E_u = \frac{(\sigma_1 - \sigma_0)}{(\varepsilon_1 - \varepsilon_0)} \tag{2}$$

where σ_1 and ε_1 are the stress and strain values of the previous maximum strain point and σ_0 and ε_0 are the stress and strain values of the next initial strain point.

We need to use a mathematical model to represent the changing law of elastic modulus. The mathematical model of variable elastic modulus is as follows.

$$E_{av} = E_0 - (E_0 - E_a)\left[1 - e^{\left(-\xi\varepsilon_0^p\right)}\right] \tag{3}$$

where E_0 is the initial elastic modulus; E_{av} is the average elastic modulus during deformation; E_a is the material parameter; ξ is the material parameters that control the rate of decrease of elastic modulus.

Based on the above formula, we fit the experiment data. The parameters E_0, E_a, and ξ in each direction are shown in Table 3.

Figure 7 shows the comparison between the experimental data points and the fitted curve. The elastic modulus in the three directions of RD, DD, and TD showed a significant downward trend with the increase of plastic strain. We find that the elastic modulus decreases faster before 3.3% plastic strain; after 3.3% plastic strain, the downward trend gradually flattens out and finally becomes a constant value. When the plastic strain is 8.3%, the elastic modulus of the rolling direction decreases by 18.9%, the elastic modulus of the diagonal direction decreased by 22.39%, and the elastic modulus of the transverse direction decreased by 20%. It can be seen from the figure that the curve fitted according to the mathematical model is very close to the experimental data. It shows that the mathematical model of variable elastic modulus can accurately describe the change law of elastic modulus of Ti-6Al-4V titanium alloy. The elastic modulus of Ti-6Al-4V titanium alloy changes in the three directions the same. However, due to the certain anisotropy of the initial elastic modulus, the elastic modulus of the RD is always greater than the elastic modulus in the other two directions during the entire deformation process. When plastic strain is large, the elastic modulus is 10 GPa larger than the other two directions.

Table 2 Material parameters of Ti-6Al-4V titanium alloy obtained from uniaxial tensile test

Direction	Elastic modulus E_0/GPa	0.2% Offset yield strength σ_s/MPa	Ultimate tensile strength σ_U/MPa	Total elongation /%	Plastic strain ratio
RD	120.4	1034	1161	12.3	2.49
DD	113.5	849	939	13.8	3.75
TD	110.0	930	1165	11.7	3.07

Table 3 Variable elastic modulus mathematical model parameters

Direction	E_0/GPa	E_a/GPa	ξ
RD	120.4	91.18	87.93
DD	113.5	88.91	84.02
TD	110.0	89.14	102.26

4 YLD200-2D yield criterion

Ti-6Al-4V titanium alloy exhibits strong anisotropy during the forming process, and the isotropic yield criterion is not applicable, so this paper will adopt the YLD2000-2D yield criterion. The YLD2000-2D yield criterion is a plane yield criterion based on plane stress. It uses two linear transformations on the Cauchy stress tensor to introduce the anisotropic parameters of the material into the yield function. The YLD2000-2D yield criterion can well describe the yield behavior of Ti-6Al-4V titanium alloy, and it is also very suitable for studying the V-shape bending springback process of thin sheet.

The YLD2000-2D yield function expression is as follows.

$$\phi = \phi' + \phi'' = 2\overline{\sigma} \tag{4}$$

where

$$\phi' = \left|X_1' - X_2'\right|^a, \tag{5}$$

$$\phi'' = \left|2X_2'' + X_1''\right|^a + \left|2X_1'' + X_2''\right|^a \tag{6}$$

where X_1', X_2', X_1'', X_2'' are the stress principal value of X' and X''.

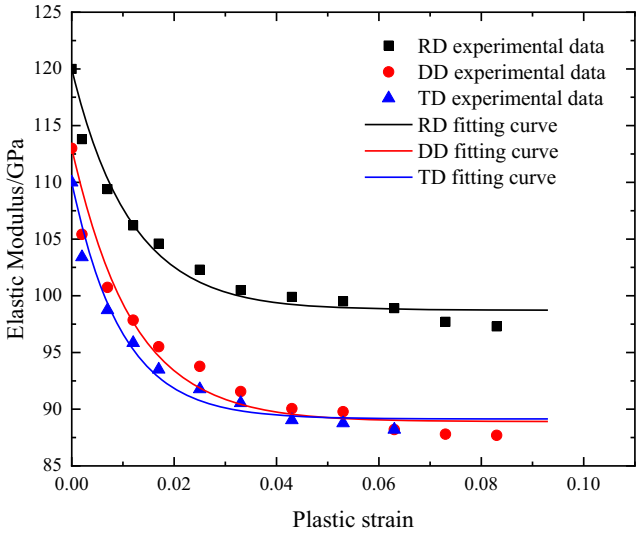

Fig. 7 Variable elastic modulus fitting curve for RD, DD, TD

$$X_1 = \frac{1}{2}\left(X_{xx} + X_{yy} + \sqrt{\left(X_{xx} + X_{yy}\right)^2 + 4X_{xy}^2}\right) \tag{7}$$

$$X_2 = \frac{1}{2}\left(X_{xx} + X_{yy} - \sqrt{\left(X_{xx} + X_{yy}\right)^2 + 4X_{xy}^2}\right) \tag{8}$$

The components of X' and X'' can be obtained by the following two linear transformations.

$$X' = C's = C'T\sigma = L'\sigma \tag{9}$$

$$X'' = C''s = C''T\sigma = L''\sigma \tag{10}$$

$$T = \begin{bmatrix} \frac{2}{3} & -\frac{1}{3} & 0 \\ -\frac{1}{3} & \frac{2}{3} & 0 \\ 0 & 0 & 1 \end{bmatrix} \tag{11}$$

The function of transformation matrix T is to transform Cauchy stress σ into the corresponding deviator stress tensor s. The function of matrices C' and C'' is to introduce anisotropic parameters.

$$\begin{bmatrix} X_{xx}' \\ X_{yy}' \\ X_{xy}' \end{bmatrix} = \begin{bmatrix} C_{11}' & C_{12}' & 0 \\ C_{21}' & C_{22}' & 0 \\ 0 & 0 & C_{66}' \end{bmatrix} \begin{bmatrix} s_{xx} \\ s_{yy} \\ s_{xy} \end{bmatrix} \tag{12}$$

$$\begin{bmatrix} X_{xx}'' \\ X_{yy}'' \\ X_{xy}'' \end{bmatrix} = \begin{bmatrix} C_{11}'' & C_{12}'' & 0 \\ C_{21}'' & C_{22}'' & 0 \\ 0 & 0 & C_{66}'' \end{bmatrix} \begin{bmatrix} s_{xx} \\ s_{yy} \\ s_{xy} \end{bmatrix} \tag{13}$$

$$\begin{bmatrix} X_{xx}' \\ X_{yy}' \\ X_{xy}' \end{bmatrix} = \begin{bmatrix} L_{11}' & L_{12}' & 0 \\ L_{21}' & L_{22}' & 0 \\ 0 & 0 & L_{66}' \end{bmatrix} \begin{bmatrix} \sigma_{xx} \\ \sigma_{yy} \\ \sigma_{xy} \end{bmatrix} \tag{14}$$

$$\begin{bmatrix} X_{xx}'' \\ X_{yy}'' \\ X_{xy}'' \end{bmatrix} = \begin{bmatrix} L_{11}'' & L_{12}'' & 0 \\ L_{21}'' & L_{22}'' & 0 \\ 0 & 0 & L_{66}'' \end{bmatrix} \begin{bmatrix} \sigma_{xx} \\ \sigma_{yy} \\ \sigma_{xy} \end{bmatrix}, \tag{15}$$

where

$$\begin{bmatrix} L_{11}' \\ L_{12}' \\ L_{21}' \\ L_{22}' \\ L_{66}' \end{bmatrix} = \begin{bmatrix} \frac{2}{3} & 0 & 0 \\ -\frac{1}{3} & 0 & 0 \\ 0 & -\frac{1}{3} & 0 \\ 0 & \frac{2}{3} & 0 \\ 0 & 0 & 1 \end{bmatrix} \begin{bmatrix} \alpha_1 \\ \alpha_2 \\ \alpha_7 \end{bmatrix}, \tag{16}$$

$$\begin{bmatrix} L_{11}'' \\ L_{12}'' \\ L_{21}'' \\ L_{22}'' \\ L_{66}'' \end{bmatrix} = \frac{1}{9}\begin{bmatrix} -2 & 2 & 8 & -2 & 0 \\ 1 & -4 & -4 & 4 & 0 \\ 4 & -4 & -4 & 1 & 0 \\ -2 & 8 & 2 & -2 & 0 \\ 0 & 0 & 0 & 0 & 9 \end{bmatrix} \begin{bmatrix} \alpha_3 \\ \alpha_4 \\ \alpha_5 \\ \alpha_6 \\ \alpha_8 \end{bmatrix}, \tag{17}$$

Table 4 Anisotropic parameters of YLD2000-2D

YLD2000-2D	α_1	α_2	α_3	α_4	α_5	α_6	α_7	α_8	a
	0.9057	1.2511	0.9941	0.9906	0.9716	0.9674	1.057	1.0942	12

where α_1 to α_8 are eight anisotropic parameters. When the value of 8 parameters is equal to 1, the yield criterion becomes an isotropic yield criterion. These 8 parameters need to be calculated from the 8 experimental data σ_0, σ_{45}, σ_{90}, σ_b, r_0, r_{45}, r_{90}, $r_b$measured by uniaxial tensile experiment and biaxial tensile experiment, among them, two experimental data σ_b and r_b are given according to Reference 15. Please refer to Reference [12] for the specific calculation method of 8 parameters. Table 4 shows the eight parameter values when $a = 12$.

5 Numerical simulation

In this paper, Abaqus finite element analysis software is used to simulate the V-shaped bending of Ti-6Al-4V titanium alloy sheet. The numerical simulation is divided into three groups, corresponding to different bending angles of 60°, 75°, and 90°. The sizes of upper die, lower die, and bending stroke are shown in Fig. 8. The numerical simulation is divided into three analysis steps. The first step is that the indenter contacts the upper layer of the sheet. The second step is to bend to the specified angle. The third step is to lift the pressure head and the sheet to rebound.

The three-dimensional model of finite element simulation of Ti-6Al-4V titanium alloy sheet V-shaped bending is shown in Fig. 9. Ti-6Al-4V titanium alloy sheet is 250 mm long, 80 mm wide, and 2 mm thick. Both the upper die and the lower die are set as discrete rigid bodies. In order to reduce the calculation time and increase the calculation efficiency, we set the sheet as a deformable shell.

Abaqus software has a high degree of openness. When the existing material model contained in the Abaqus material library cannot accurately represent the material behavior to be simulated, it provides users with a convenient custom material model subroutine interface, namely Umat subroutine interface. In this paper, a constitutive model of Ti-6Al-4V titanium alloy material is established based on the above YLD2000-2D yield criterion and variable elastic modulus mathematical model and embed the model into Abaqus software through the Umat subprogram interface. In order to study the influence of the yield criterion and the variable elastic modulus on the prediction of the springback of Ti-6Al-4V, this paper conducts bending springback simulations for three different constitutive models.

In order to accurately describe the hardening curve of Ti-6Al-4V titanium alloy, this paper chooses the Voce model to describe the change of its flow stress. We fitted the flow stress of the rolling direction, and the fitting result is as follows.

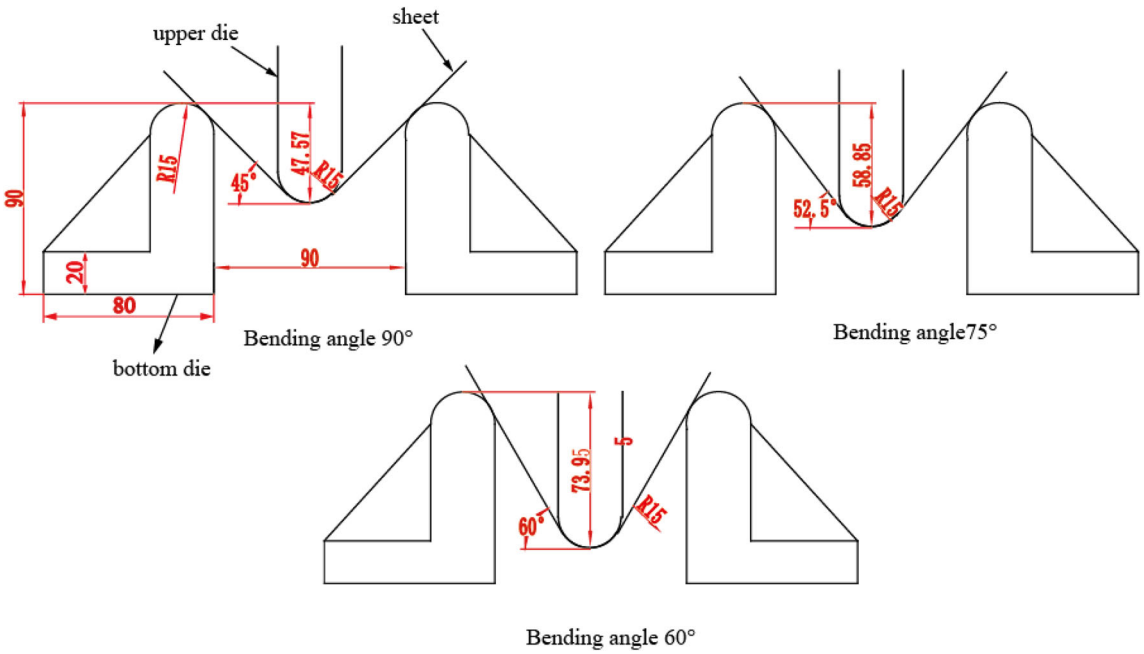

Fig. 8 Schematic diagram of mold size and bending stroke

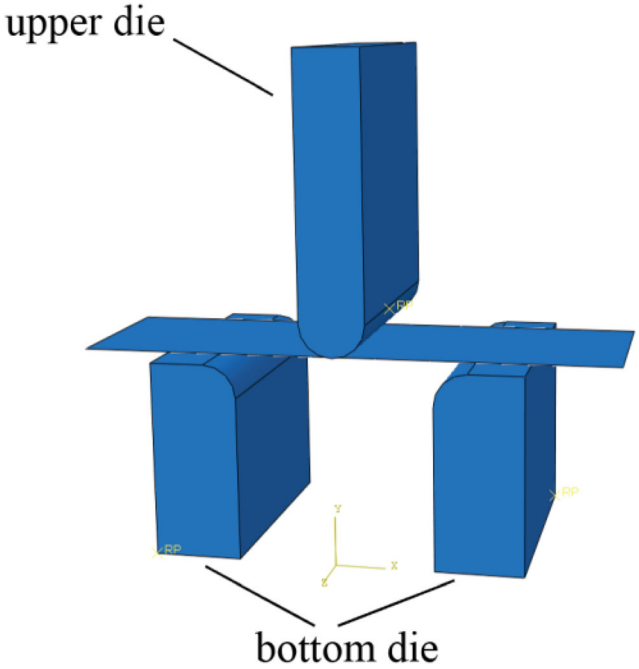

Fig. 9 Finite element model

$$\sigma_s = 1065 + 470.8\left[1-e^{-4.935\bar{\varepsilon}^{p}}\right] \tag{18}$$

The material parameter settings of each constitutive model in the numerical simulation are shown in Table 5.

In the numerical simulation of V-shaped bending of Ti-6Al-4V titanium alloy sheet, the element type of the sheet is selected as the S4R four-node shell element. We divide the sheet into three areas and set different element sizes. The areas with large deformation are more finely divided, and the areas with small deformation are more rough. In this way, it increases the accuracy of the calculation results without affecting the calculation speed. The element division of the sheet is shown in Fig. 10.

Figure 11 shows that the transverse elastic strain cloud diagram of the sheet at a bending angle of 60° calculated by "YLD2000-2D + variable elastic modulus" constitutive model. SDV1 represents the elastic strain. It can be seen that the Ti-6Al-4V titanium alloy sheet has obvious springback after unloading. During the bending process, the area of elastic deformation is mainly concentrated in the middle area of the sheet, and the elastic strain is fully restored after unloading.

6 Bending test and springback analysis

6.1 V-shaped bending test

In order to verify the accuracy of the numerical simulation results, the V-shaped bending test of Ti-6Al-4V titanium alloy sheet was carried out on a universal electronic testing machine. As shown in Fig. 12, firstly, we contact the upper die with the sheet surface, then set the stroke down corresponding to the bending angle in the operating system, and finally lift up the upper die. The die size as shown in Fig. 8. The geometrical parameters of Ti-6Al-4V titanium alloy sheet used in the experiment are 250 mm*80 mm*2 mm.

Figure 13 shows that the final formed shape of the sheet of three groups of V-shaped bending experiments. Figure 14 shows the change curve of springback angle with different pre-bending angles. We find that when the pre-bending angle increases, the springback angle decreases. The calculation formula of springback angle is as follows:

Table 5 Input parameters of three constitutive models

Material parameters	Constitutive model		
	YLD2000-2D+ Variable elastic modulus	YLD2000-2D+ Constant elastic modulus	Isotropic
α_1	0.9057	0.9057	—
α_2	1.2511	1.2511	—
α_3	0.9941	0.9941	—
α_4	0.9906	0.9906	—
α_5	0.9716	0.9716	—
α_6	0.9674	0.9674	—
α_7	1.057	1.057	—
α_8	1.0942	1.0942	—
E_0	120.4	120.4	120.4
E_a	91.18	—	—
ξ	87.93	—	—
ν	0.36	0.36	0.36

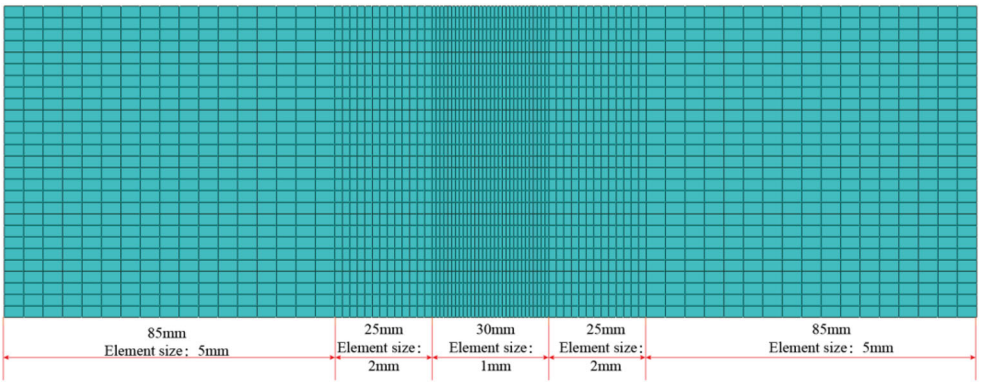

Fig. 10 Element division method

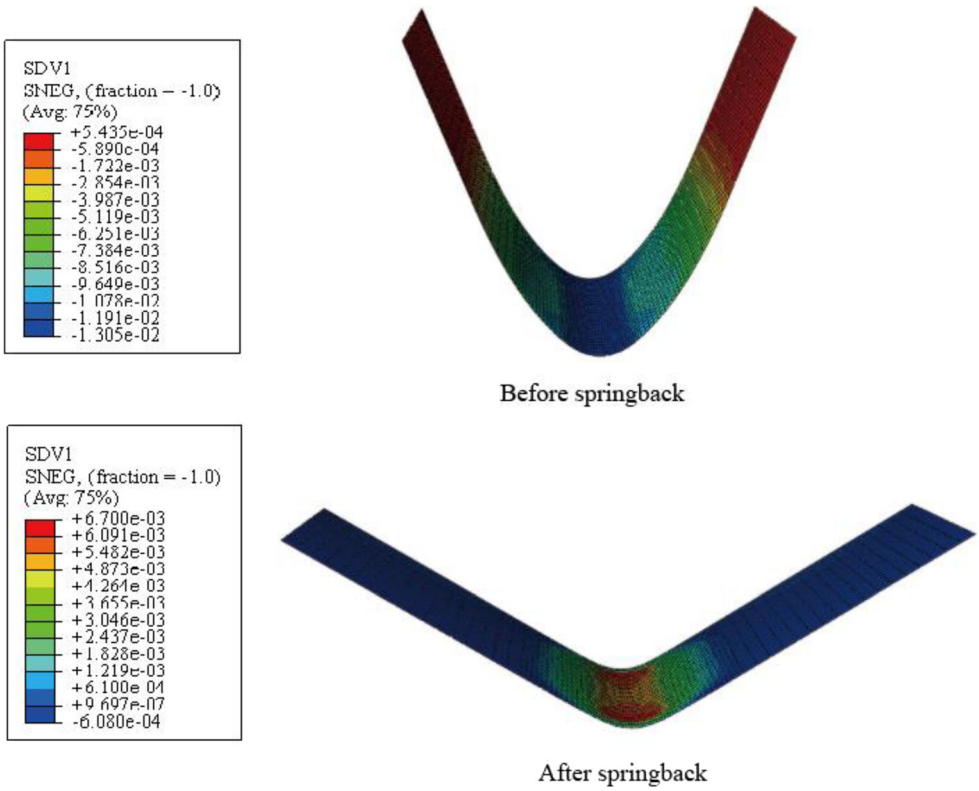

Fig. 11 Numerical simulation of transverse elastic strain cloud at a bending angle of 60°

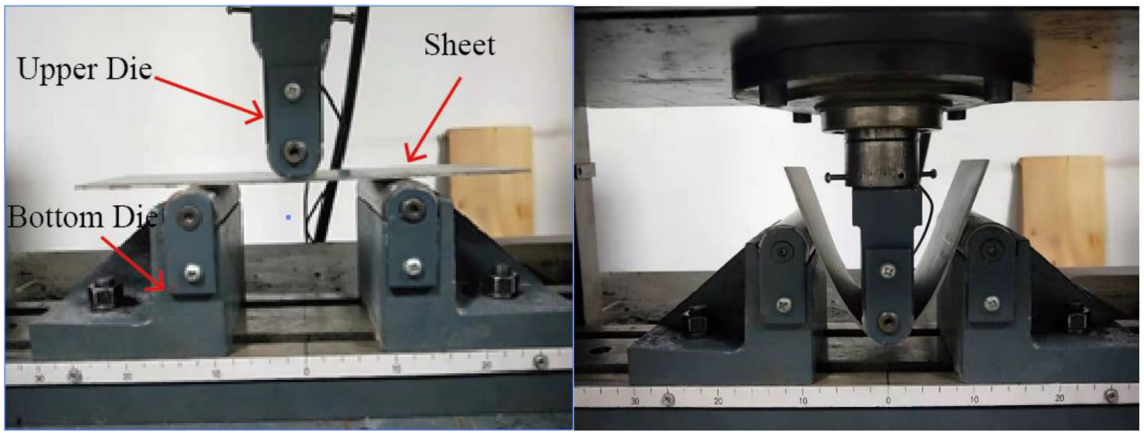

Fig. 12 V-shaped bending experiment process diagram

Fig. 13 The final formed shape of the sheet

$$\theta_s = \frac{180-\theta_b}{2} - \theta_e \tag{19}$$

where θ_s is the springback angle; θ_b is the pre-bending angle. θ_e is the angle between the plate and the horizontal line after springback.

6.2 Analysis of springback prediction accuracy

Through numerical simulation and bending experiment, we obtained the springback situation of Ti-6Al-4V titanium alloy sheet under different bending angles and different material constitutive models. The influence of different material constitutive models on the prediction of V-shaped bending springback of Ti-6Al-4V titanium alloy sheet is shown in Fig. 15. The figure shows the influence of different material constitutive models on the final forming effect of sheet under three different pre-bending angles of 60°, 75°, and 90°. When the pre-bending angles are 60°, 75°, and 90°, the included angles between the sheet and the horizontal plane after bending springback are respectively 30.85°, 26.76°, and 21.81°. Under the condition of the same pre-bending angle, the numerical simulation results based on the isotropic constitutive model have the biggest difference from the experimental results, and the numerical simulation results based on YlD2000-2D yield criterion and variable elastic modulus material constitutive model are the closest to the experimental results.

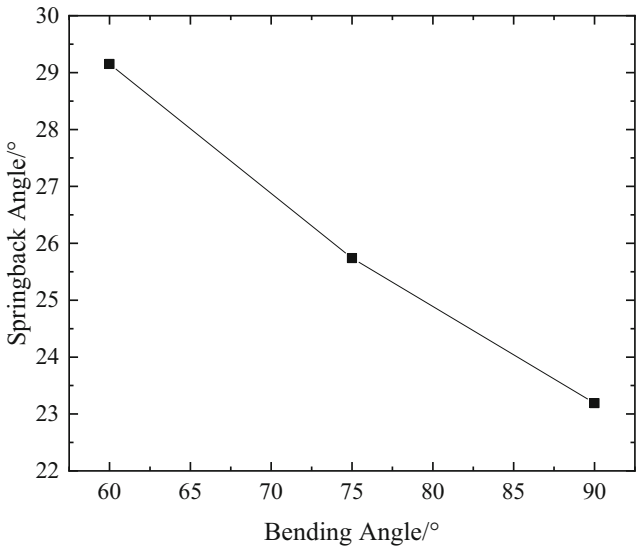

Fig. 14 Springback angle of different pre-bending angles

As shown in Fig. 16, it shows that the predicted springback angle of different constitutive models at pre-bending angle of 60°, 75°, and 90°. The constitutive model based on YLD2000-2D yield criterion and variable elastic modulus has higher prediction accuracy than the other two constitutive models. Under the case of 60° pre-bending angle, the prediction accuracy of springback is 12.3% higher than isotropic constitutive model and 8.6% higher than constant elastic modulus constitutive model. Under the case of 75° pre-bending angle, the prediction accuracy of springback is 14.6% higher than isotropic material constitutive model and 10.2% higher than constant elastic modulus material constitutive model. Under the case of 90° pre-bending angle, the prediction accuracy of springback is 12.3% higher than isotropic material constitutive model, and 8.8% higher than constant elastic modulus material constitutive model. In conclusion, the material constitutive model based on YLD2000-2D and variable elastic modulus can significantly improve the springback prediction accuracy of V-shaped bending of Ti-6Al-4V titanium alloy sheets.

7 Conclusion

This article takes Ti-6Al-4V titanium alloy as the research object. Based on the numerical simulation, the influence of the yield criterion and the change of elastic modulus on the prediction accuracy of the V-shaped bending springback of Ti-6Al-4V titanium alloy sheet was studied, and the following conclusions were drawn:

(1) According to the uniaxial quasi-static tensile test, we found that the yield strength and elastic modulus of Ti-

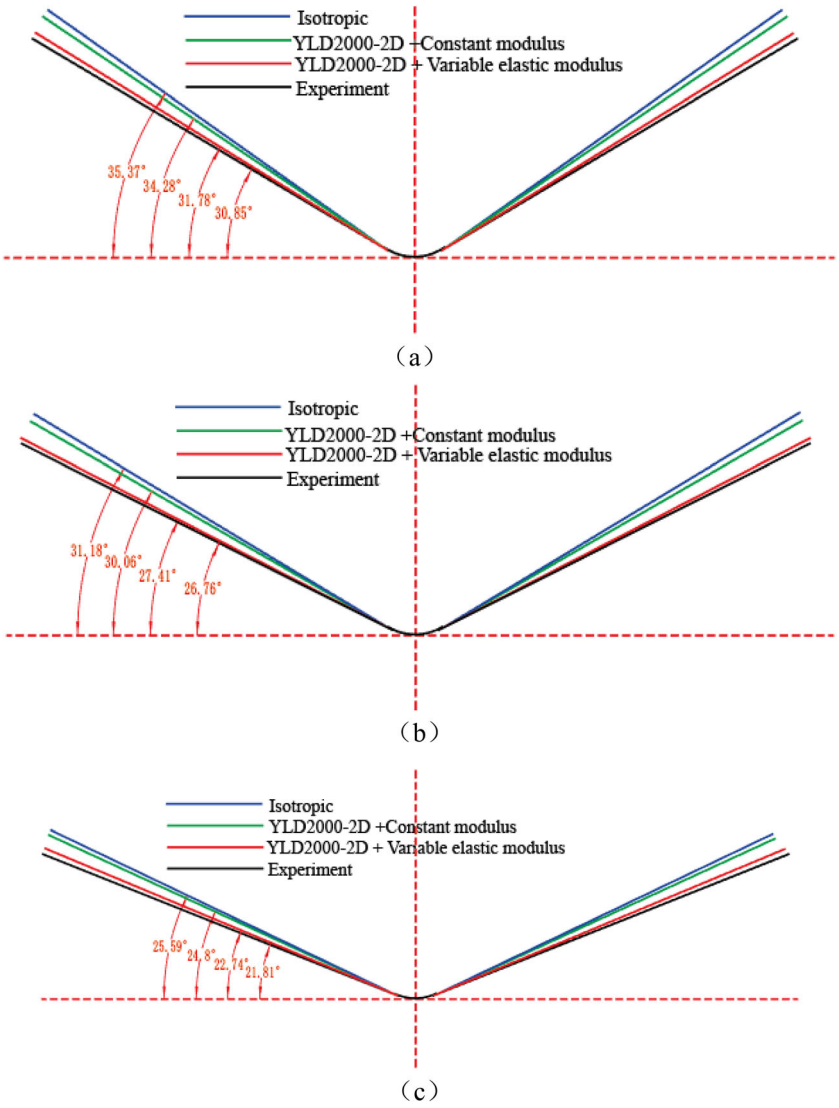

Fig. 15 Numerical simulation and experimental results based on different constitutive models. **a** Pre-bending angle 90°. **b** Pre-bending angle 75°. **c** Pre-bending angle 60°

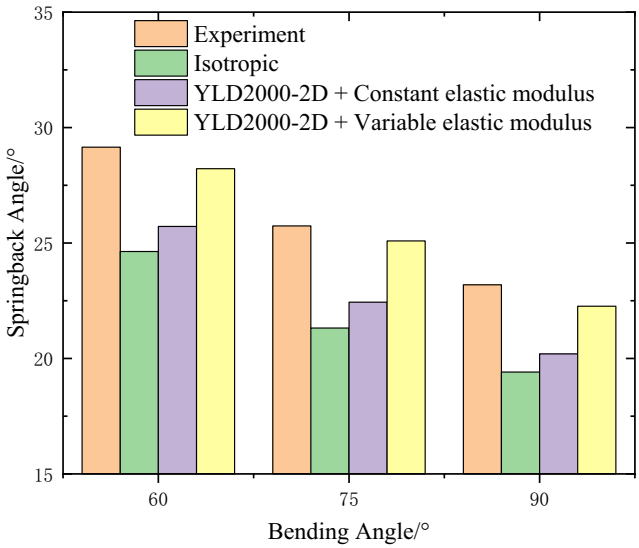

Fig. 16 Differences in springback prediction of different constitutive models at a pre-bending angle of 60°, 75°, and 90°

6Al-4V titanium alloy had obvious anisotropy in the three directions of RD, DD, and TD. Among them. The yield stress in the DD direction was the lowest, and the yield stress in the RD direction was the highest. The elastic modulus in the RD direction was the highest, and the elastic modulus in the TD direction was the lowest.

(2) Based on the cycle loading-unloading-loading experiment, we found that the elastic modulus of Ti-6Al-4V titanium alloy decreases with the increase of plastic strain and finally becomes a fixed value. Based on the above rules, a mathematical model of the variable elastic modulus of Ti-6Al-4V titanium alloy was established.

(3) Based on YLD2000-2D yield criterion and variable elastic modulus mathematical model, a constitutive model that can accurately reflect the anisotropy of Ti-6Al-4V material and its variable elastic modulus characteristics was established.

(4) Comparing the numerical simulation results under three different constitutive models and the V-bending springback test results of Ti-6Al-4V titanium alloy sheet, we concluded that the constitutive model based on YLD2000-2D yield criterion and variable elastic modulus significantly improved the springback prediction accuracy of numerical simulation, which was 14.6% higher than that of the isotropic constitutive model.

Author contribution Zijian Liu and Lidong Ma contributed to the conception of the study. Zijian Liu, Lidong Ma, Yukang Du, and Peiyu Liu performed the experiment. Zijian Liu, Lidong Ma, and Zhijuan Meng contributed significantly to analysis and manuscript preparation. Zhijuan Meng performed the data analyses. Zijian Liu and Lidong Ma wrote the manuscript.

Funding This work was supported by National Natural Science Foundation of China (grant number 52004169), Applied Basic Research Programs of Shanxi Province (grant numbers 201901D111244, 201901D211311), Major Science and Technology Projects of Shanxi Province (grant number 2020xxx009).

Data availability The data used to support the findings of this study are available from the corresponding author upon request.

Declarations

Ethics approval Not applicable

Consent to participate Not applicable

Consent for publication Not applicable

Competing interests The authors declare that they have no conflicts of interest.

References

1. Moiseyev VN (2005) Titanium alloys: Russian aircraft and aerospace applications. CRC Press.
2. Gurrappa I (2003) Characterization of titanium alloy Ti-6Al-4V for chemical, marine and industrial applications. Mater Charact 51(2): 131–139
3. Schauerte O (2003) Titanium in automotive production. Adv Eng Mater 5(6):411–418
4. Zong Y, Liu P, Guo B, Shan D (2015) Springback evaluation in hot v-bending of Ti-6Al-4V alloy sheets. Int J Adv Manuf Technol 76(1-4):577–585
5. Zhao J, Yin J, Ma R, Ma L (2011) Springback equation of small curvature plane bending. Science China Technol Sci 054(009): 2386–2396
6. Jun Z, Xue ZR, Ping QZ, Rui M (2013) A study on springback of profile plane stretch–bending in the loading method of pretension and moment. Int J Mech Sci 75(10):45–54
7. Jun ZM, Xue ZR (2014) Prediction and control of springback in setting round process for pipe-end of large pipe. Int J Pres Pei ZP, Rui Vess Pipi 116:56–64
8. Ma L, Ma H, Liu Z, Chen S (2019) Theoretical analysis of five-point bending and springback for preforming process of ERW pipe FFX forming.Math. Probl Eng 11:1703739
9. Liu C, Yue T, Li D (2019) A springback prediction method for a cylindrical workpiece bent with the multi-point forming method. Int J Adv Manuf Technol 101(1-3):2571–2583
10. Wu Y, Zhao Y (2014) Cold bending forming and springback analysis of high-strength steel thick plates. China Ship Build 55(04):33–47
11. Barlat F, Lian J, Baudelet B (1989) A yield function for orthotropic sheets under plane stress conditions. Strength Metals Alloys 1:283–288
12. Barlat F, Brem JC, Yoon JW, Chung K, Dick RE, Lege DJ, Pourboghrat F, Choi S-H, Chu E (2003) Plane stress yield function for aluminum alloy sheets-part 1: theory. Int J Plast 19(9):1297–1319
13. Naofal J, Naeini HM, Mazdak S (2019) Effects of hardening model and variation of elastic modulus on springback prediction in roll forming. Metals 9(9):1005
14. Jung J, Jun S, Lee HS, Kim BM, Lee MG, Kim JH (2017) Anisotropic hardening behaviour and springback of advanced high-strength steels. Metals 7(11):480
15. Badr OM, Barlat F, Rolfe B, Lee MG, Weiss M (2016) Constitutive modelling of high strength titanium alloy Ti-6Al-4 V for sheet forming applications at room temperature. Int J Solids Struct 80: 334–347
16. Badr OM, Rolfe B, Hodgson P, Weiss M (2015) Forming of high strength titanium sheet at room temperature. Mater Design 66(Feb.):618–626
17. Badr OM, Rolfe B, Weiss M (2018) Effect of the forming method on part shape quality in cold roll forming high strength Ti-6Al-4V sheet. J Manuf Process 32:513–521
18. Yang XM, Dang LM, Wang YQ, Zhou J, Wang BY (2020) Springback prediction of tc4 titanium alloy v-bending under hot stamping condition TC4. J Cent South Univ 27(9):2578–2591
19. Mulidrán P, Spiák E, Tomá M, Roha V, Stachowicz F (2020) The springback prediction of deep - drawing quality steel used in V - bending process. Acta Mech Slovaca 23(4):14–18
20. Mulidrán P, Spiák E, Tomá M, Slota J, Majerníková J (2020) Numerical prediction and reduction of hat-shaped part springback made of dual-phase ahss steel. Metals 10(9):1119
21. Morestin F, Boivin M (1996) On the necessity of taking into account the variation in the Young modulus with plastic strain in elastic-plastic software. Nucl Eng Des 162(1):107–116
22. Yoshida F, Uemori T, Fujiwara K (2002) Elastic-plastic behavior of steel sheets under in-plane cyclic tension-compression at large strain. Int J Plast 18(5-6):633–659
23. Liu X, Cao J, Chai X, Liu J, Zhao R, Kong N (2017) Investigation of forming parameters on springback for ultra high strength steel considering Young's modulus variation in cold roll forming. J Manuf Process 29:289–297
24. Sun L, Wagoner RH (2011) Complex unloading behavior: nature of the deformation and its consistent constitutive representation.Int. J Plasticity 27(7):1126–1144